



Optimizing BioTac Simulation for Realistic Tactile Perception

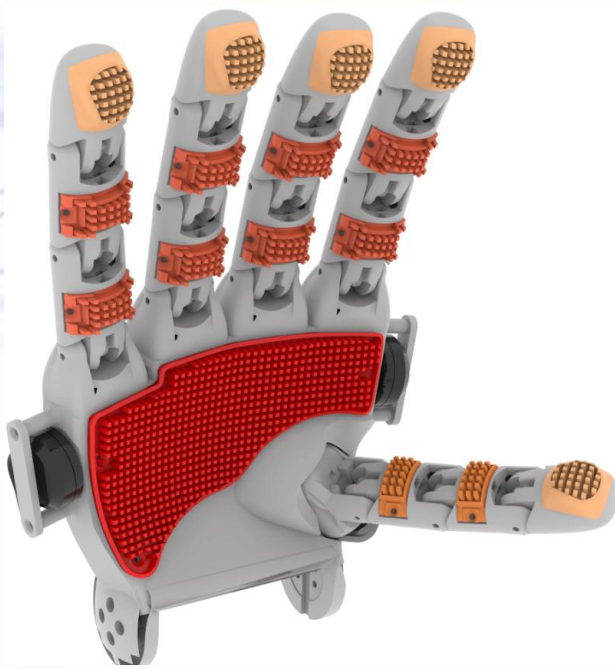
Wadhah Zai El Amri & Nicolás Navarro-Guerrero

International Joint Conference on Neural Networks (IJCNN), Yokohama, Japan, 2024.

Tactile Sensing Sensors

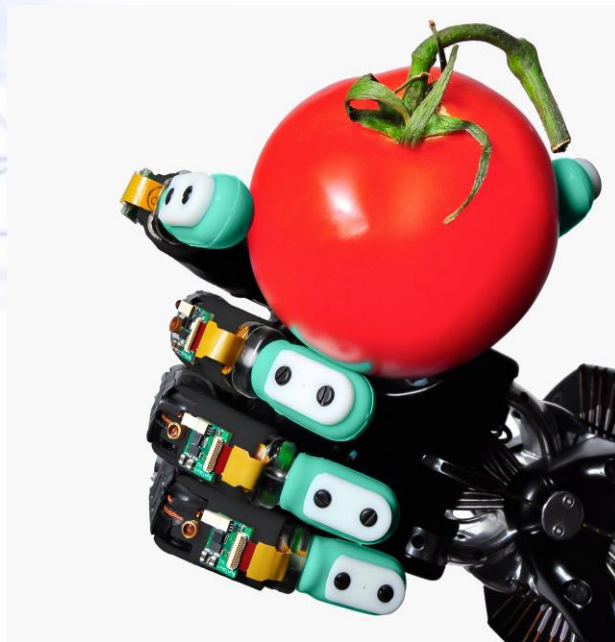
- offer robots valuable information.
- complement knowledge coming from other modalities.

Time-series-based tactile sensors



Adapted from: [source](#)

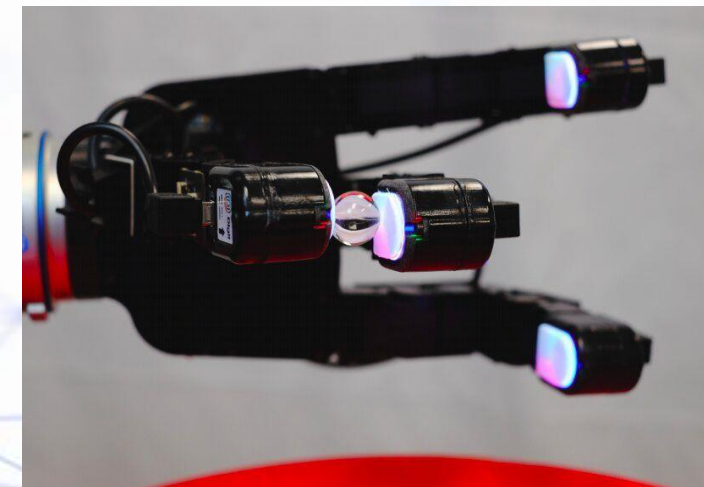
(a)



(b)

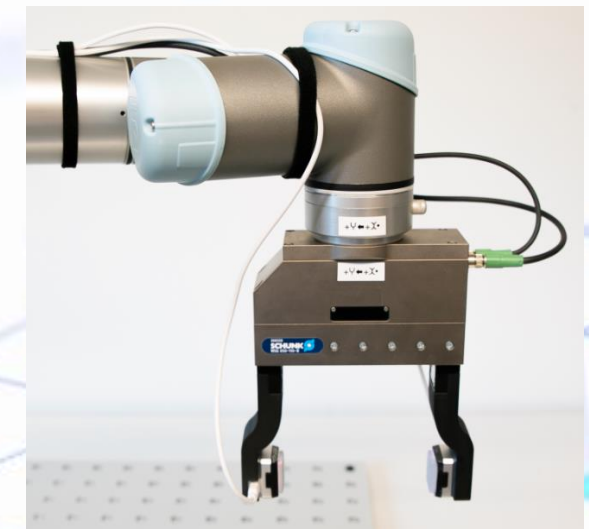
Fig. 1: Time-series-based tactile sensors: (a) RH8D hand with fingerprint patterns. (b): Shadow hand with BioTac sensors.

Vision-based tactile sensors



Adapted from: [source](#)

(a)



Adapted from: [source](#)

(b)

Fig. 2: Vision-based tactile sensors: (a) Allegro and with DIGIT sensor (b): Schunck gripper with GelSight sensors.

BioTac Sensor

- is a time-series-based tactile sensor.
- has a rigid core, covered with elastomeric skin filled with an incompressible conductive fluid.
- Has a sampling rate equal to 100 Hz.
- outputs: 19 electrode voltages $\mathbf{e}_1, \dots, \mathbf{e}_{19}$, absolute and dynamic fluid pressure \mathbf{p}_{dc} and \mathbf{p}_{ac} , temperature \mathbf{t}_{dc} and heat flow \mathbf{t}_{ac} .

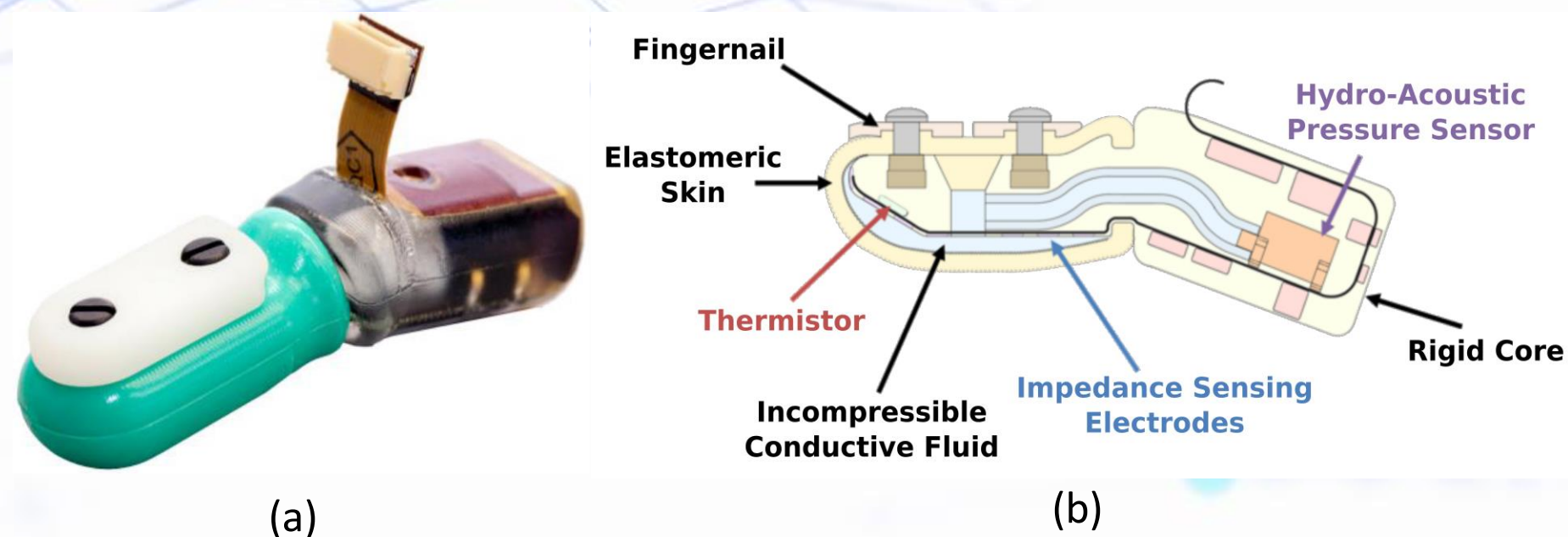


Fig. 3: (a): BioTac 2P Sensor [1]. (b): Internal Section of the BioTac Tactile Sensor [1].

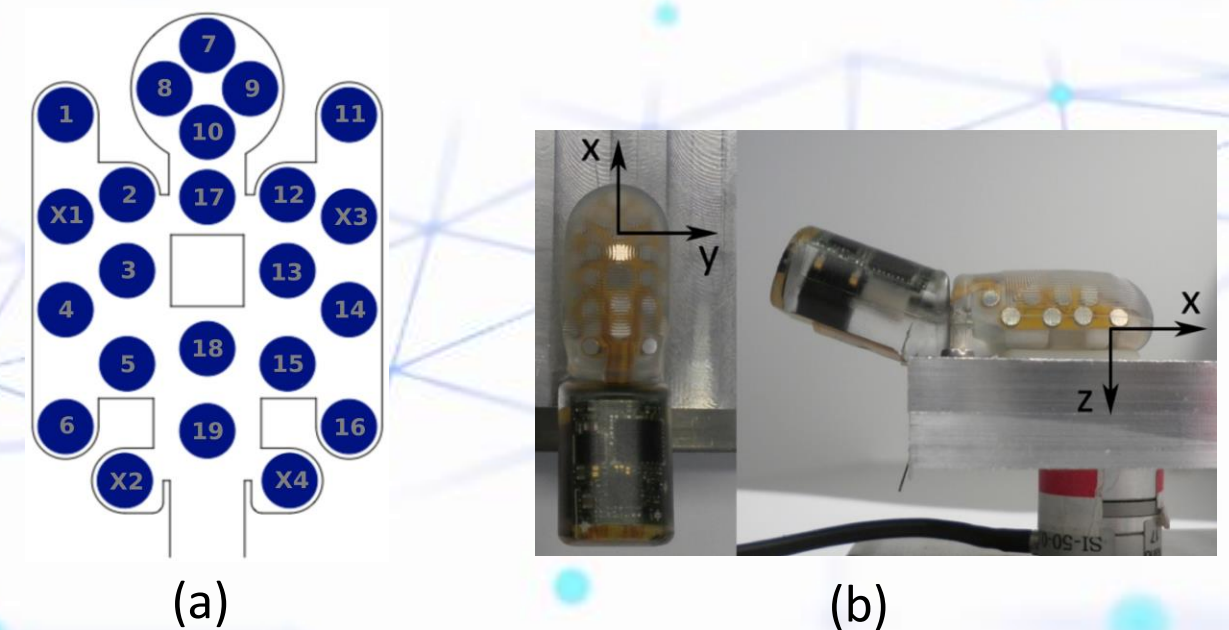


Fig. 4: (a): Map of the electrodes on the BioTac sensor [2]. (b): BioTac sensor and the position/orientation of the coordinate frame [2].

Motivation

- Sensor is unavailable.
- Experiment repetitions are costly.

→ Simulate the BioTac sensor.

- The simulation should be:
 - Reliable.
 - Accurate
 - Real-time capable.

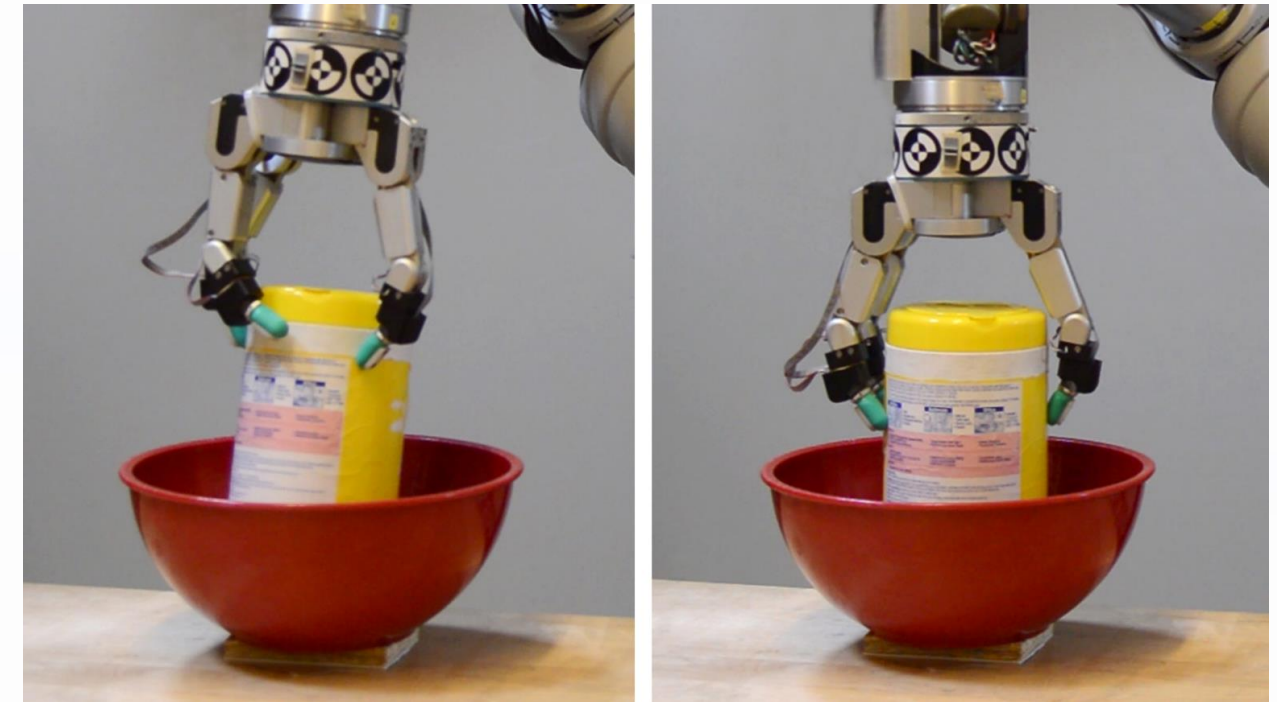


Fig. 5: Dataset collection procedure [3].

Adapted from: [source](#)

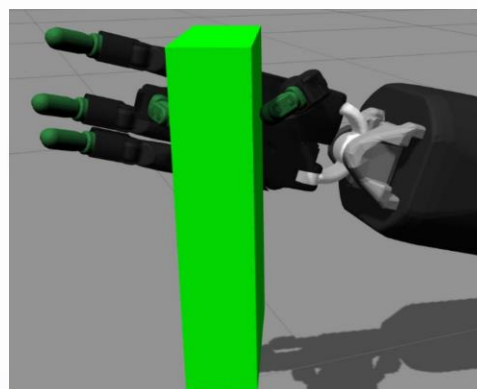
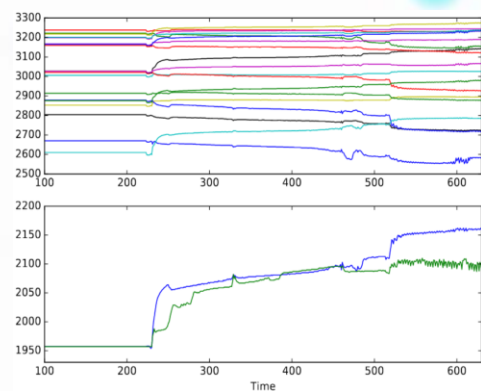


Fig. 6: Real setup and simulation [5].

Existing BioTac Sensor Simulations

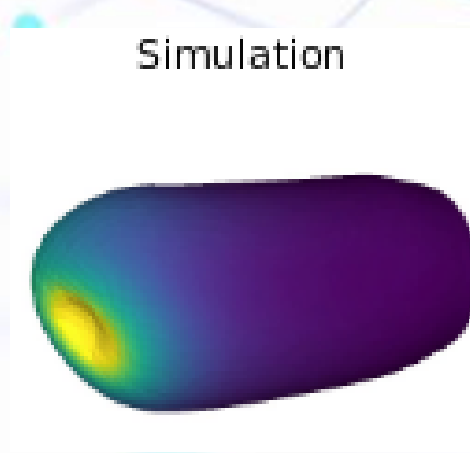
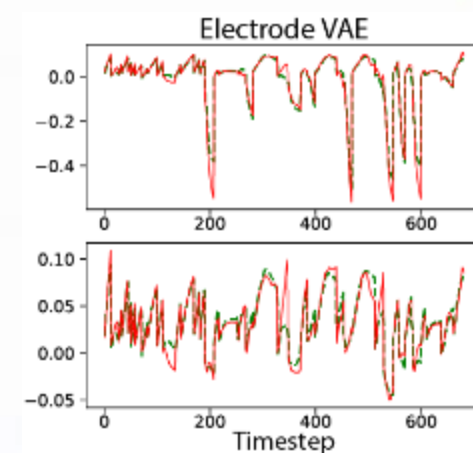
Ruppel et al. [4]

- Based on rigid-body simulation.
- A feed-forward neural network that predicts the sensor outputs.
- Requires using the temperature values in the input vector.



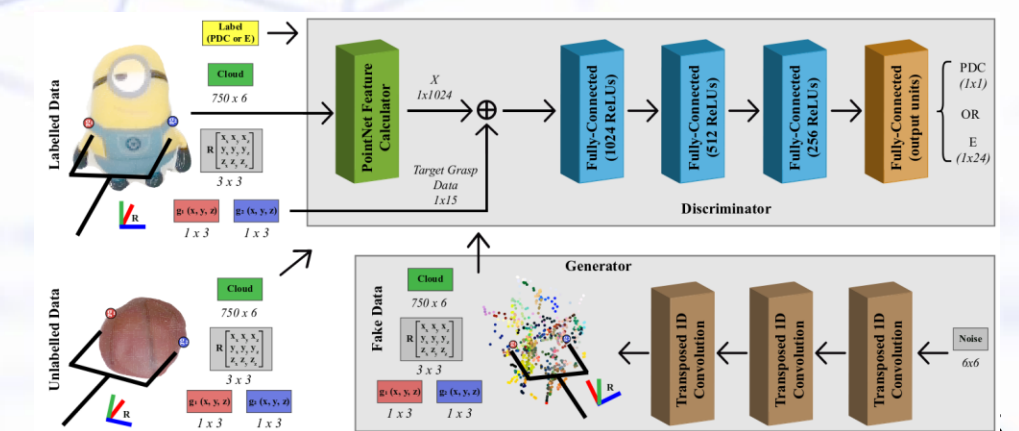
Narang et al. [5]

- Based on soft-body simulation.
- Uses a VAE to predict the electrode outputs from the deformation mesh.
- Pressure and vibration signals are not recorded.
- Can not be used in real-time systems.



Zaoata-Impata and Gil [6]

- Uses vision to estimate the electrode values.
- Uses a modified Semi Regression Generative Adversarial Network (SR-GAN).
- Small dataset (4000 samples).
- Vibration signals are not recorded.



Investigating Ruppel's Simulation [4]

Used Dataset:

- ca. 1h of interaction with an indenter with a spherical tip of radius equal to 2 mm, attached to a calibrated force-torque sensor.
- Approximately 290K BioTac readings with the corresponding force values and 3D indenter-tip's positions.

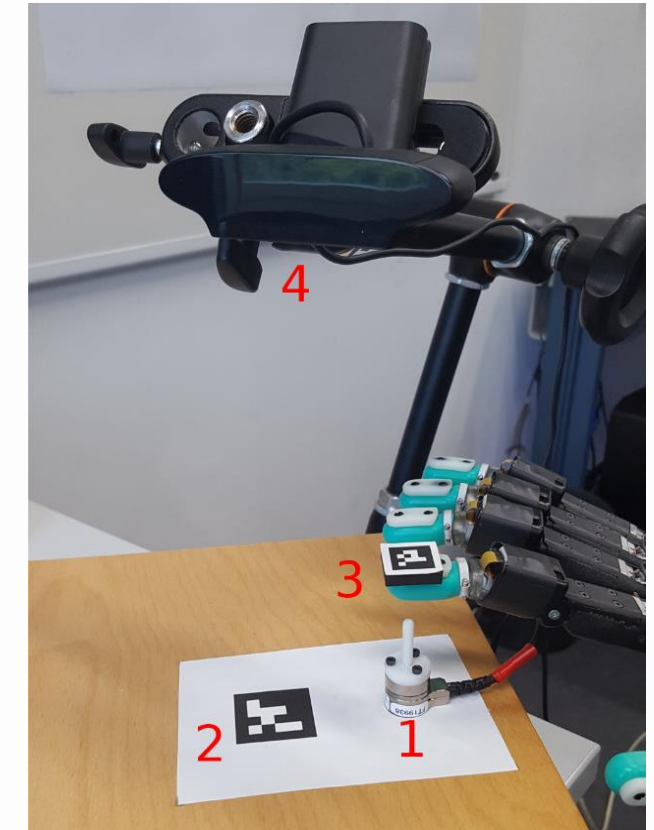


Fig. 7: Experiment setup [4].

Trained Network:

- Input Vector:
 - Position: \mathbf{x} , \mathbf{y} , and \mathbf{z} at $t = T$,
 - Forces: \mathbf{F}_x , \mathbf{F}_y , and \mathbf{F}_z at T , $T-10$, and $T+10$,
 - BioTac Temperature readings at $t = T$.
- Three separate dense layer columns that merge into a dense layer.

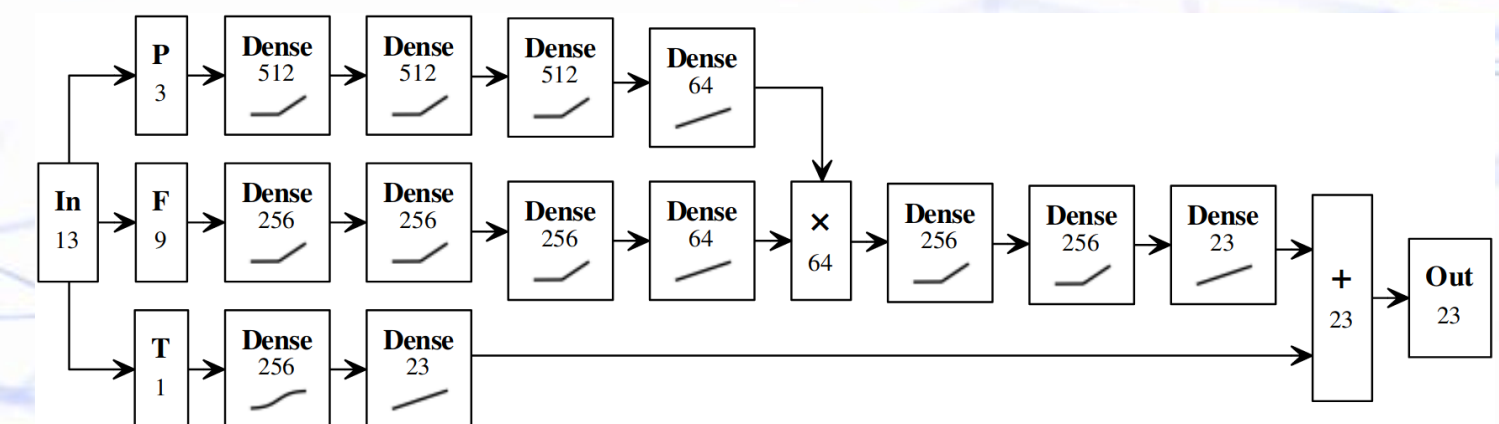


Fig. 8: Deep neural network architecture for simulating BioTac sensor outputs [4].

Investigating Ruppel et al. Simulation [4]

Investigating the Training with Temperature Readings

- Temperature values are not present in simulation:
 - Ruppel et al. suggest fixing it to the mean temperature value, when deploying.
- We conduct 10-fold cross-validation:

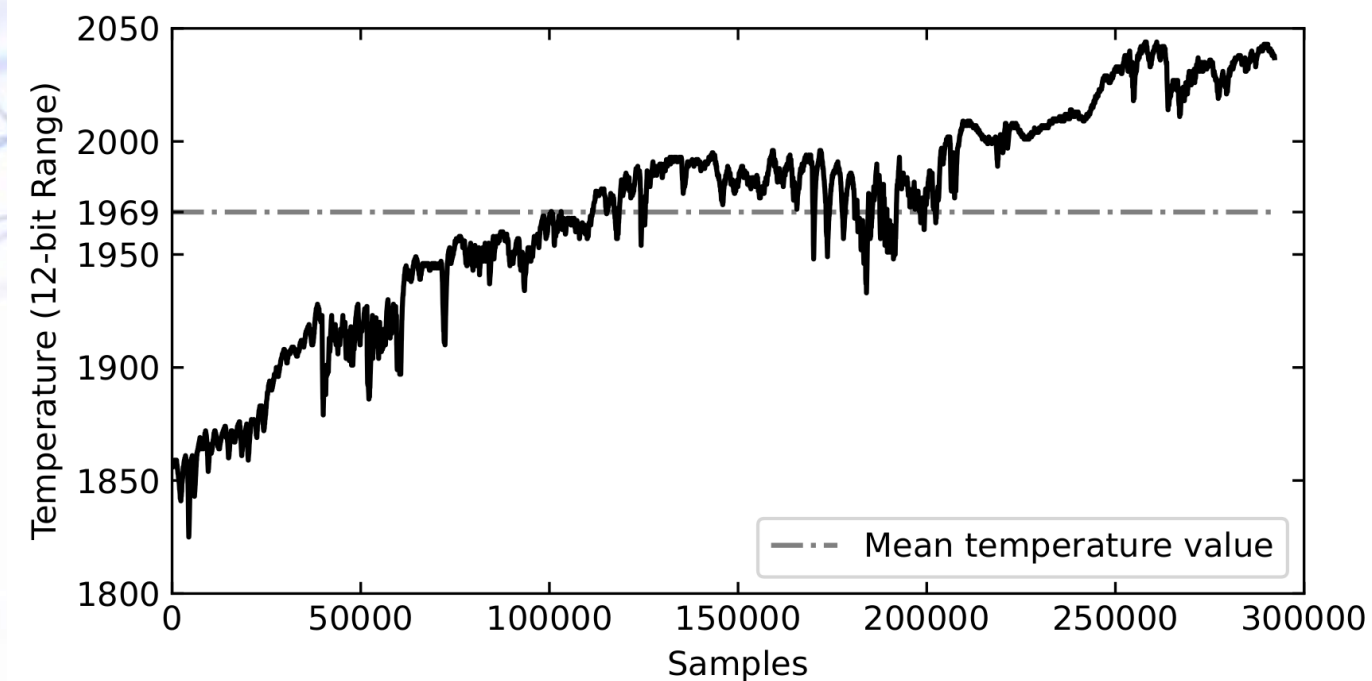


Fig. 9: Temperature values of the BioTac sensor in the Ruppel et al. [4]'s dataset.

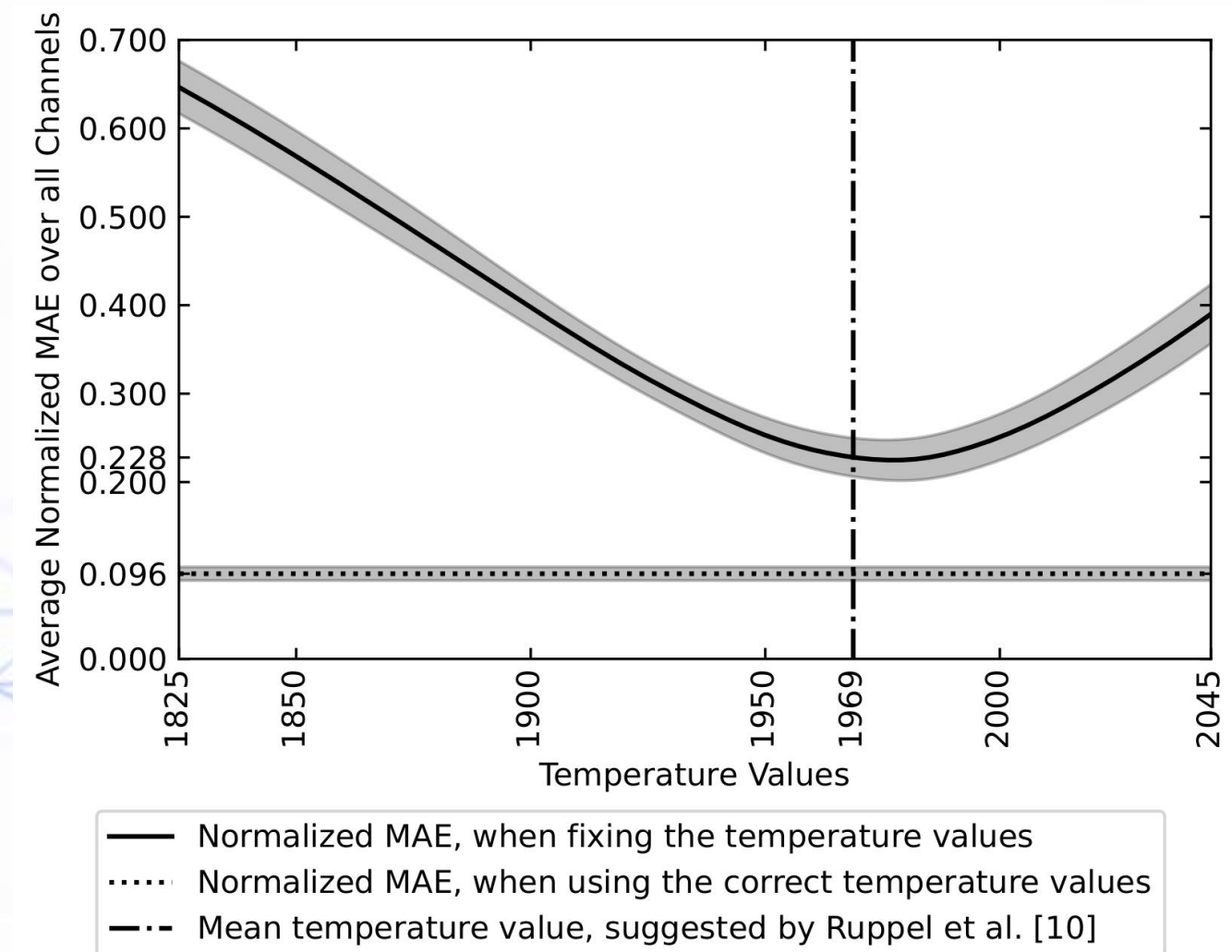


Fig. 10: Average normalized MAE over all channels for ten folds for the baseline Network.

Experiments

Training without Temperature Readings

- We propose three different networks:
- The input vector includes:
 - Position: \mathbf{x} , \mathbf{y} , and \mathbf{z} at $t = T$,
 - Forces: \mathbf{F}_x , \mathbf{F}_y , and \mathbf{F}_z at T , $T-10$, and $T+10$.
- The output vector includes:
 - 19 electrode voltages $\mathbf{e}_1, \dots, \mathbf{e}_{19}$ at $t = T$,
 - Absolute and dynamic fluid pressure: \mathbf{p}_{dc} and \mathbf{p}_{ac} at $t = T$.

XGBoost Regressor

- Fast and suitable for predicting continuous output variables.
- We use multi-regressors: one for each output channel.
- SMAC3 [8] is used to find the best hyperparameters.

Feed-Forward Neural Network

- Commonly used in regression tasks.
- SMAC3 [8] is used to find the best hyperparameters.

Transformer Encoder

- Proved beneficial in several time-series tasks.
- Based on ViT encoder.
- SMAC3 [8] is used to find the best hyperparameters.

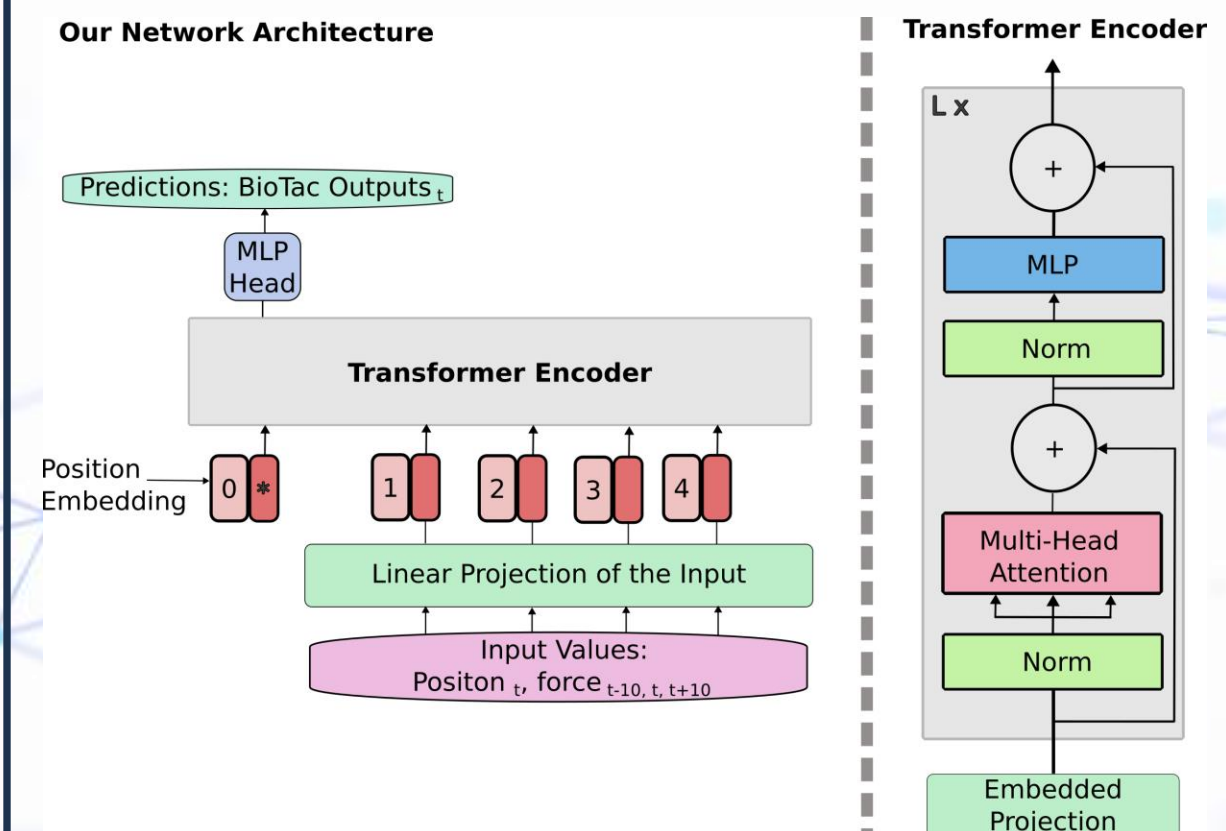


Fig. 11: Visualization of our used transformer architecture, based on Dosovitskiy et al. [9].

Experiments

Training without Temperature Readings

- XGBoost Regressor achieves the lowest error.
- The transformer encoder achieves comparable results with a low number of parameters.

Table 1: Results of all trained network over all ten folds.

	Nb. Param.	MAE	Norm. MAE	MAE	Norm. MAE
		Over all Channels		Electrodes Only	
Ruppel et al. [10]	806K	18.977 (1.719)	0.228 (0.022)	17.147 (1.642)	0.232 (0.023)
Our XGBoost Regressor	1584K	13.368 (1.340)	0.150 (0.014)	11.446 (1.204)	0.150 (0.015)
Our Feed-Forward Neural Network	2233K	14.693 (1.386)	0.168 (0.015)	12.724 (1.252)	0.169 (0.016)
Our Transformer Encoder	599K	13.760 (1.400)	0.156 (0.016)	11.736 (1.280)	0.155 (0.016)

Experiments

Training without Temperature Readings

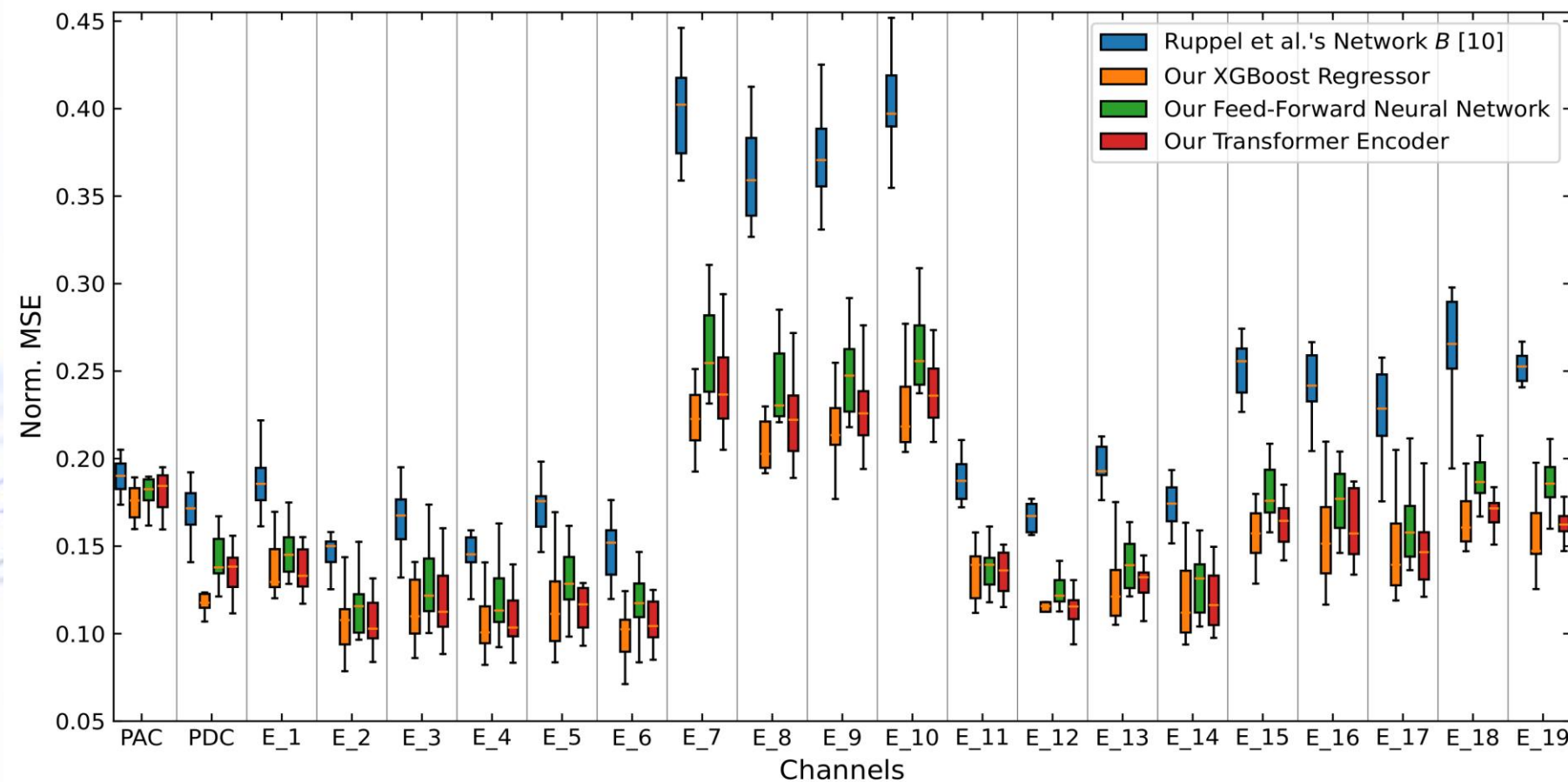
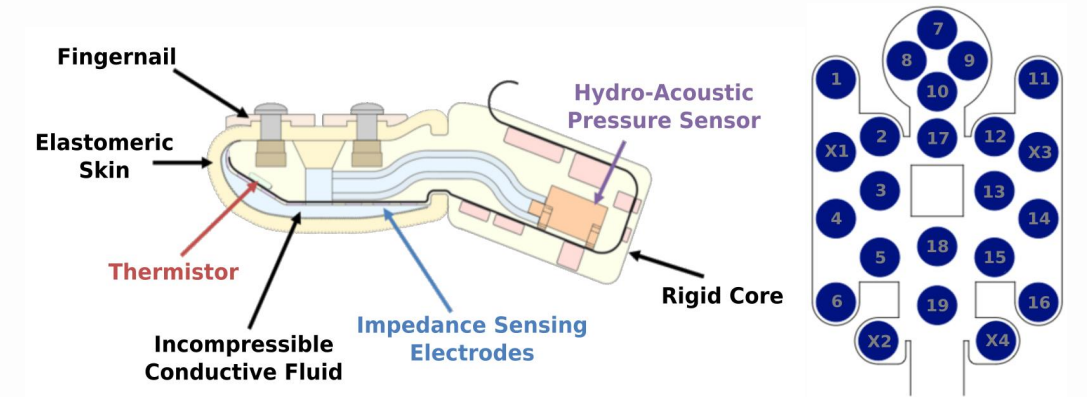


Fig. 12: Distribution of the normalized MAE for each channel and all models.

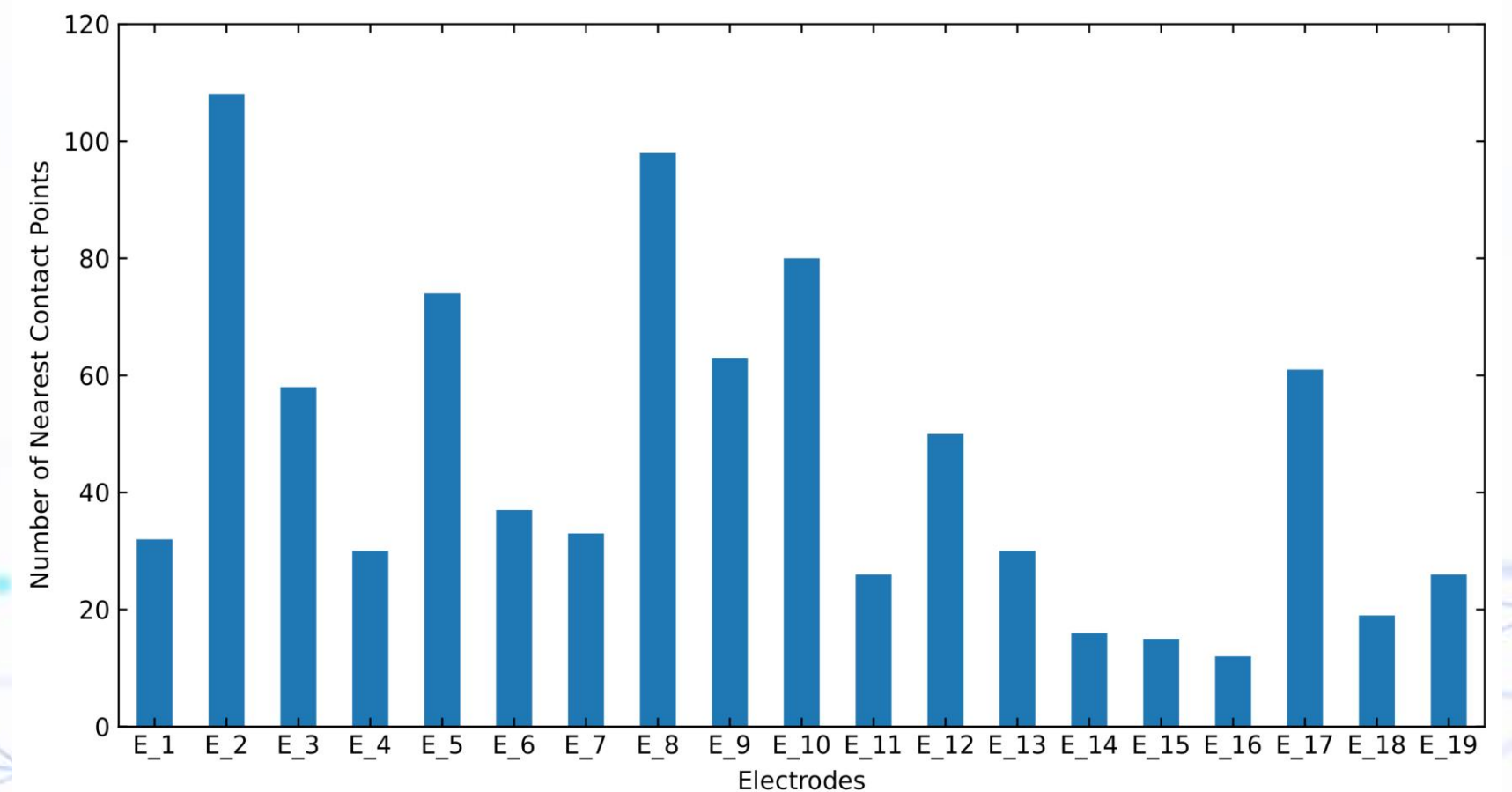


Fig. 13: Distribution of nearest contact points for each electrode.

- Non-uniform distribution of the number of touches near each electrode, implying an unbalanced dataset.
- The BioTac sensor does not have radial symmetry.
- The fluid volume is not the same throughout the sensor. Particularly near electrodes 7, 8, 9, and 10.

Experiments

Varying the Windowing Size

- Investigate the following input combinations:
 1. Forces F_t : $\forall t \in \{T, T - 10, T + 10\}$.
 2. Forces F_t : $\forall t \in \{T, T - 10\}$.
 3. Forces F_t : $\forall t \in \{T\}$.
 4. Forces F_t : $\forall t \in \{T, T - 10, T - 5, T + 5, T + 10\}$.
 5. Forces F_t : $\forall t \in [T - 10, T + 10], t \in \mathbb{N}$.
 6. Forces F_t : $\forall t \in [T - 10, T], t \in \mathbb{N}$.
 7. Current, last, and next position and forces F_t : $\forall t \in \{T, T - 10, T + 10\}$.
 8. Current, last, and next position and forces F_t : $\forall t \in [T - 10, T + 10], t \in \mathbb{N}$.

Experiments

Varying the Windowing Size

- Investigate the following input combinations:
 1. Forces F_t : $\forall t \in \{T, T - 10, T + 10\}$.
 5. Forces F_t : $\forall t \in [T - 10, T + 10], t \in \mathbb{N}$.
 7. Current, last, and next position and forces F_t : $\forall t \in \{T, T - 10, T + 10\}$.
 8. Current, last, and next position and forces F_t : $\forall t \in [T - 10, T + 10], t \in \mathbb{N}$.

Table 2: Significance test with the corrected paired t-Test [7].

	5 vs 1	7 vs 1	8 vs 1
Our XGBoost Regressor	0.282% (0.999)	-0.055% (0.190)	-0.208% (0.009)
Our Feed-Forward Neural Network	0.217% (0.715)	0.862% (0.961)	0.402% (0.758)
Our Transformer Encoder	0.077% (0.631)	0.188% (0.672)	-0.662% (0.047)

→ The error improvement is small. However, it is statistically significant.

→ Including last and next position adds valuable information, when combined with shorter force intervals.

Experiments

Varying the Windowing Size

Table 3: Significance test with the corrected paired t-Test [7].

vs	Our XGBoost Our FFNN	Our XGBoost Our Transformer	Our Transformer Our FFNN
1	-1.778% (0.000)	-0.531% (0.074)	-1.247% (0.002)
2	-1.360% (0.001)	-0.259% (0.250)	-1.101% (0.000)
3	-1.272% (0.003)	0.851% (0.996)	-2.123% (0.000)
4	-1.989% (0.000)	-0.032% (0.459)	-1.956% (0.000)
5	-1.279% (0.002)	-0.173% (0.322)	-1.107% (0.002)
6	-1.106% (0.003)	0.092% (0.616)	-1.197% (0.002)
7	-2.696% (0.000)	-0.774% (0.105)	-1.921% (0.000)
8	-2.389% (0.001)	-0.077% (0.439)	-2.312% (0.002)

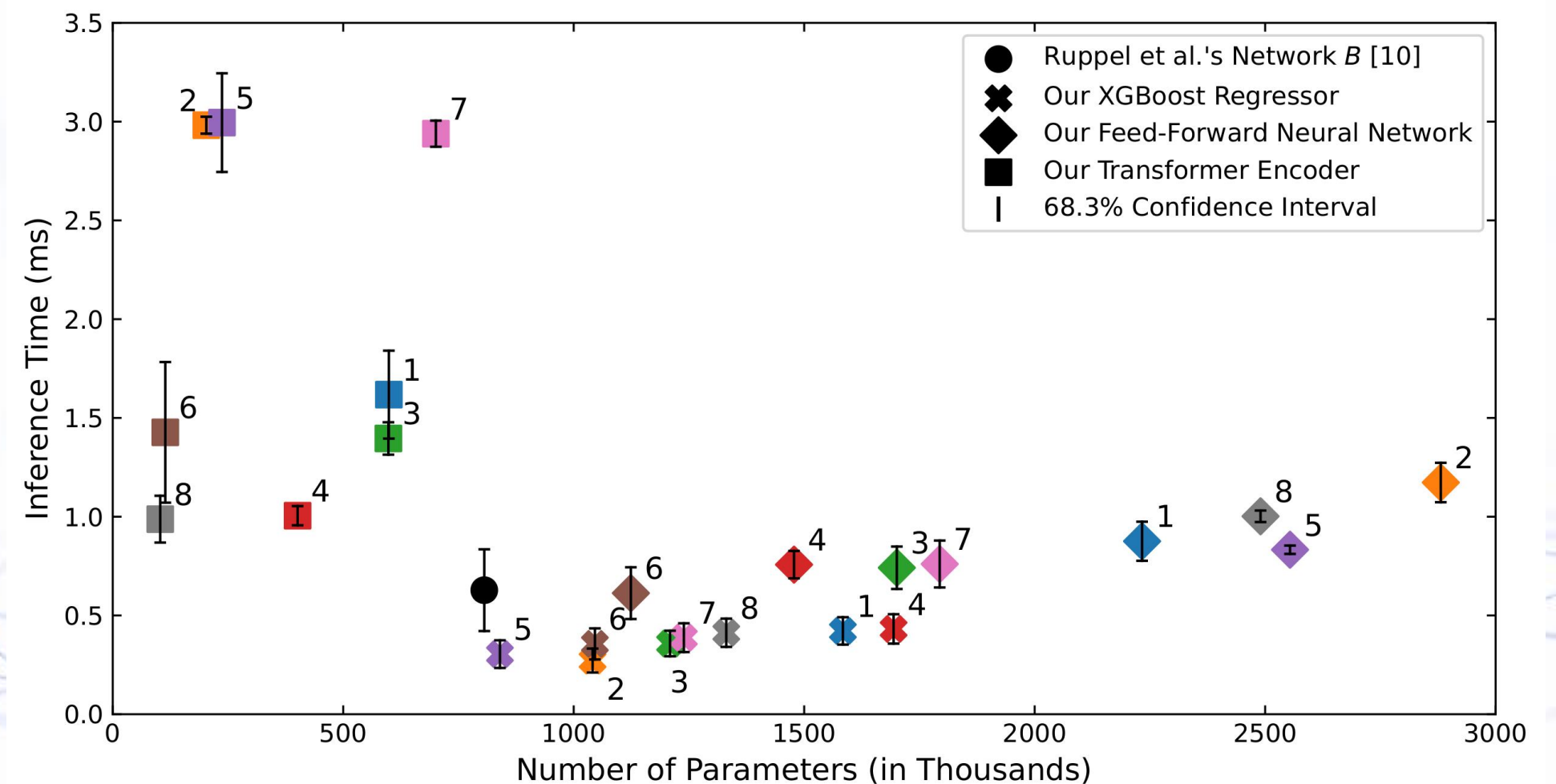


Fig. 14: Visualization of inference time against the number of parameters for each model over all input combinations.

- There is not statistical significance difference between XGBoost Regressor and Transformer Network.
- Transformers have less parameters. However, they have higher inference time.

Conclusion

Our Contribution:

- We include a thorough analysis of Ruppel et al.'s work [4].
- We introduced three alternative models, that are independent of the temperature readings, resulting in an absolute error reduction of 8.0%, and a relative error improvement of 14.9%.
- We report on the limitations of the dataset. Particularly, the dataset is unbalanced and only includes a single indenter type.

Future Work:

- Extend the dataset and transfer it to a soft-body simulation, i.e., Isaac Gym.
- Transfer the BioTac dataset to other sensor modalities.
For example: **time-series-based modality** ↔ **vision-based modality**.

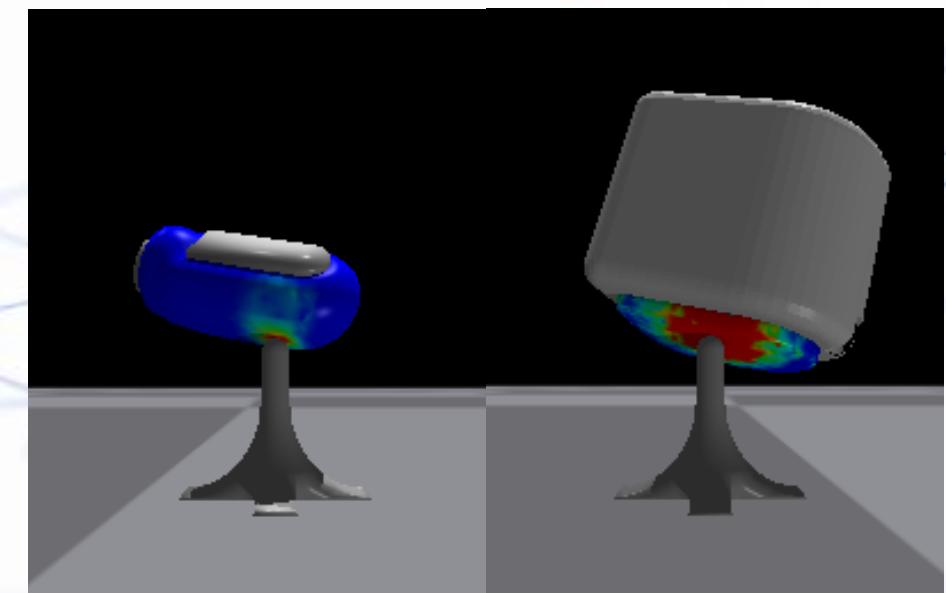


Fig. 15: Dataset collection environment for BioTac and DIGIT sensor.

Contact



Wadhah Zai El Amri



wadhah.zai@l3s.de



www.l3s.de



@l3s_luh



@l3s-research-center



@forschungszentruml3s



@l3s-research-center